Sources of oscillation frequency rise with rising solar activity

W. A. Dziembowski
Warsaw University Observatory and Copernicus Astronomical Center,Poland
and

P. R. Goode
Big Bear Solar Observatory, New Jersey Institute of Technology, Big Bear City, 92314, USA
pgoode@bbso.njit.edu

ABSTRACT

We analyze and interpret SOHO/MDI data on the variations of oscillation frequency changes between 1996 and 2004 focusing on differences between activity minimum and maximum of solar cycle 23. We study only the behavior of the centroid frequencies, which reflect changes averaged over spherical surfaces. Both the f-mode and p-mode frequencies are correlated with general measures of the sun's magnetic activity. However, the physics behind each of the two correlations is quite different. We show that for the f-modes the dominant cause of the frequency increase is the dynamical effect of the rising magnetic field. The relevant rise must occur in subphotospheric layers reaching to some 0.5 - 0.7 kG at a depth of about 5 Mm. However, these implied constraints also require the field change in the atmosphere to be so small that it has only a tiny dynamical effect on p-mode frequencies. For p-modes, the most plausible explanation of the frequency increase is a decrease of less than 2% in the radial component of the turbulent velocity in the outer layers. Lowering velocity implies lowering efficiency of the convective transport, hence lower temperature, which also contributes to the p-mode frequency increase.

Subject headings: Sun : Helioseismology, solar variability

1. Introduction

We now have data on the evolution of solar oscillation frequencies covering nearly

all of solar cycle 23. Information about cycle-dependent changes in solar oscillations includes data on the mean multiplet frequencies, $\bar{\nu}_{\ell n}$, the multiplet structures described by the $a_{k,\ell n}$ coefficients, corresponding mode amplitudes and widths. In this paper, we focus on changes in the $\bar{\nu}$.

The correlation between p-mode frequencies and the magnetic activity cycle was first observed during the declining phase of the cycle 21 (Woodard & Noyes, 1985) and confirmed during the next cycle by a number of independent studies (Libbrecht & Woodard 1990; Woodard et al. 1991; Bachmann & Brown 1993; Elsworth et al. 1994; Regulo et al. 1994; Chaplin et al. 1998). The increase of f-mode frequencies with rising activity was discovered during the rising phase of the current cycle.

The physical origin of oscillation frequency increases with rising activity has been a matter of controversy. The first explanation, given by Goldreich et al. (1991, hereafter GMWK), was that the dominant cause of frequency growth with activity is the effect of an averaged small scale magnetic field changing the frequencies directly through the perturbed Lorentz force and indirectly through the induced pressure change. An objection to this explanation was raised by Kuhn (2000) who argued that direct measurements of the rms field in the sun's photosphere (Lin, 1995; Lin & Rimmele, 1999) exclude the field growth required in this picture. Instead, he proposed that the main effect causing p-mode frequency rise is a decrease in turbulent velocity due to the rising field's inhibition of convection, which is believed to be the main effect of the magnetic field on the sun's interior structure (e.g. Spruit, 2000).

As for the f-modes, Antia et al. (2000) first noted that the frequency rise with rising activity and that it is roughly proportional to the frequency itself. Such a behavior could be explained in terms of a solar radius decrease. The number quoted by these authors was 5 km during the three years of the rising phase of the cycle. This result was broadly confirmed by Dziembowski, Goode & Schou (2001, hereafter DGS) who analyzed SOHO/MDI data and found that the f-mode frequency shifts may be explained by two components: one being similar to that found by Antia et al. (2000), and the other growing more rapidly with frequency. DGS pointed out that the former component cannot arise from shrinking of the photospheric radius, but rather a layer located between 4 and 8 Mm beneath the photosphere. They also suggested that the shrinking is caused by increase of the radial component of a small-scale magnetic field beneath 8 Mm below the surface having a 1 -10 kG level rms value.

The result presented by DGS was criticized by Antia (2003) who argued that the signal found in SOHO/MDI could be completely accounted by annual variation of a non-solar origin. We do not agree with his criticism. However, we still regarded it useful to reconsider our interpretation having now a much larger data set in hand. Indeed, the interpretation presented in this paper is different: we now attribute the observed rise of f-mode frequencies directly to the rise of the magnetic field in the layers sampled by f -modes – that is, the outer 8 Mm.

2. Frequency changes between 1996 and 2004 from SOHO/MDI data

Libbrecht & Woodard (1990), who first determined activity related p-mode frequency shift for modes over a broad range of degrees, ℓ, noted that most of the frequency dependence of the shift is described by the inverse of the mode inertia, $I_{\ell n}$, which they called mode mass. We thus express the frequency shifts in the form

$$\Delta\bar{\nu}_{\ell n} = \frac{\gamma_{\ell n}}{\tilde{I}_{\ell n}}, \qquad (1)$$

where $\tilde{I}_{\ell n}$ is dimensionless mode inertia, which is calculated assuming a common normalization of the radial mean displacement in the photosphere. Such calculations require a solar model. In this work, we use model S of Christensen-Dalsgaard et al.(1996). The adopted normalization is such that $\tilde{I}_{10,19} = 1$. Values of $\tilde{I}_{\ell n}$ decrease with ℓ. The n-dependence is more complicated. At low n, there is a sharp decline. The maximum inertia is reached at a certain, rather high value of n (=22 at $\ell = 10$) and there is a slow decline with ever higher n. The p-mode data extend up to $\ell = 200$ and cover a frequency, ν, range of $1.1 - 4.5$ mHz. For these latter modes, the mode dependence is essentially reduced to a simple ν-dependence (see Fig. 4 in DSG). The lack of a separate ℓ-dependence tells us that the sources of frequency shift must be localized in the outer layers above the lower turning point for the modes in the sample, or at least for the modes that matter.

We emphasize that we treat the f-modes separately because even in the outer layers these modes have vastly different properties than those of p-modes at the same frequency, hence we cannot expect the same $\gamma(\nu)$ dependence for both types of modes. The kernels for calculating γ's resulting from changes in the magnetic field, turbulent pressure, and temperature calculated by Dziembowski & Goode (2004, hereafter DG) are indeed very different for these two types of modes. In the next section, we will, as in DGS, consider representations including the "radius" for f-modes, but we will argue against a significant role for it. Both types of $\gamma(\nu)$-dependence are helioseismic probes of the averaged changes over spherical surfaces in the subphotospheric layers during the activity cycle. However, they are independent probes.

The plots in Fig.1 show the frequency averaged γ's for all available datasets from SOHO/MDI measurements calculated from frequency differences relative to the first set from activity minimum of cycle 23. For the f-modes, we fitted constant (ν-independent) values for γ. For the p-mode we fitted three term Legendre polynomial series. We used all available frequencies in the two averaged sets. The frequency differences are weighted by the inverse of sum of the squared errors. The similarity in the behavior seen in the two panels might suggest that the source of the changes is the same in both cases but, as we shall see, this is not true.

3. The $\gamma(\nu)$-dependence for f- and p-modes

The ν-dependence yields a clue to the physics of frequency change. By averaging frequencies over five sets covering nearly one year of the solar minimum phase and ten sets covering two years of the maximum phase, we averaged out the annual

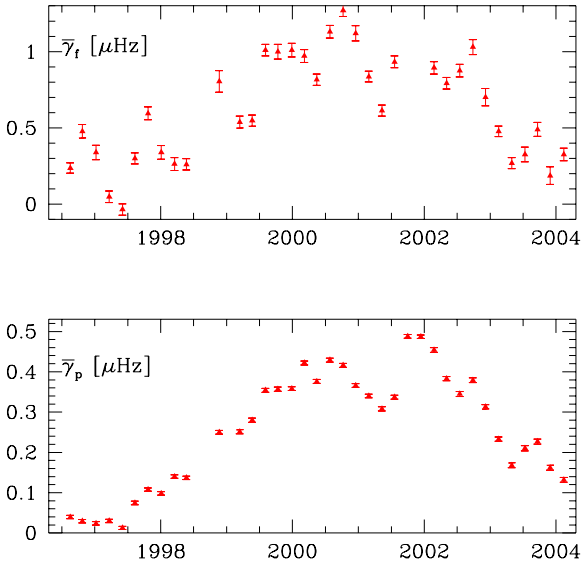

Fig. 1.— The values of the averaged γ's, which are global helioseismic measure of solar activity, are derived from 38 SOHO/MDI data sets. Note that the p-mode γ's (lower panel) very closely replicate changes in other general measures of solar activity during the cycle, showing in particular two maxima separated by some 1.4 y. The behavior of the f-modes (upper panel) is similar, but the values are less significant. The larger errors are mainly a consequence of an order of magnitude fewer f-modes.

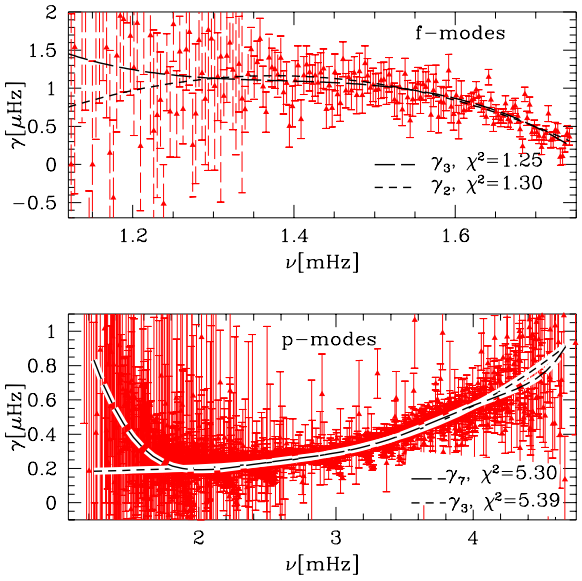

Fig. 2.— Frequency dependence of the γ's derived from the frequency difference between averaged frequencies from solar maximum phase (2000.4 - 2002.4) and the minimum phase (1996.3 - 1997.3). The lines represent fits using truncated Legendre polynomial series. Subscripts at γ's denote the order at which the series was truncated. The quoted values of χ^2 are calculated per degree of freedom

changes that are apparently non-solar in origin (DGS; Antia 2003).

Figure 2 shows individual $\gamma_{\ell n}$ values with the 1σ error bars and the Legendre polynomial fits. The fit depends on truncation order, $N_{\rm tr}$, of the polynomial, but the results stabilize at $N_{\rm tr} = 3$ for the f-modes, and $N_{\rm tr} = 7$ for p-modes.

The robust feature of the $\gamma(\nu)$ dependence for the f-modes is the gradual decrease of γ between $\nu = 1.37$ and 1.74 mHz, corresponding to the ℓ-range of 185−300. Including an ΔR_f-term representing variations of the f-mode radius does not lead to stable results. The numbers in Table 1 demonstrate the erratic behavior of ΔR_f and $\bar{\gamma}$ with increasing $N_{\rm tr}$. We thus abandon the idea that the rise of f-mode frequencies is caused by a shrinking of the radius beneath the bottom of the f-mode zone. In Section 4, we will argue that the dominant part the frequency increase is due to *in situ* rise of the magnetic field.

The robust feature of the $\gamma(\nu)$-dependence for the p-modes is the steady increase beyond $\nu = 2$ mHz. For both p- and f-modes,

Table 1: Fitting the f-mode frequency shifts to

$$\Delta\nu = -\frac{3}{2}\frac{\Delta R_f}{R}\nu + \frac{\gamma(\nu)}{\tilde{I}}$$

using the Legendre polynomial series truncated at $N_{\rm tr}$ for $\gamma(\nu)$.

$N_{\rm tr}$	ΔR_f[km]	$\bar{\gamma}$	χ^2
0	0	0.70± 0.02	3.18
1	0	1.19± 0.04	1.56
2	0	0.91± 0.06	1.30
3	0	1.06± 0.08	1.25
0	-4.79	0.41± 0.04	2.14
1	5.41	1.94± 0.15	1.39
2	-7.90	-0.50± 0.58	1.26
3	10.23	3.06± 2.60	1.26

higher frequency means a stronger sampling of the outermost layers. Therefore, the opposing behavior of the two types of modes at the high frequency end of the spectrum suggests that different physical effects are responsible for the frequency increase correlated with rising solar activity.

The smallest values of χ^2 for the p-modes are significantly higher than those for the f-modes. Undoubtedly, the relatively higher χ^2 is caused by temporal fluctuations in activity during the maximum phase (for the f-modes such fluctuations are closer to being within the relatively larger error bars). However, the relatively high χ^2 for the maximum phase with respect to the minimum might also be due to an inadequacy of the fit in which the mode dependence in $\gamma_{\ell n}$ comes only through frequency. For instance, an additional mode dependence is expected due to changes buried in the deep layers located below or near turning of certain p-modes in the sample. To check, we plot the residuals against the position of the mode turning points, as determined by

$$f_{\ell\nu} \equiv \frac{\ell + 0.5}{\nu},$$

and show the results in Fig. 3. We see that for $f_{\ell\nu} > 50$, corresponding to a turning point at a depth of about 40 Mm, the residuals are on average somewhat less than zero, while they are greater than zero for $f_{\ell\nu} < 50$. This means that a detectable contribution to the p-mode frequency changes arises in the layers reaching down to a depth of 40Mm, however most of the contribution arises in much shallower layers. Note that there is no visible contribution from the vicinity of the bottom of the convective envelope.

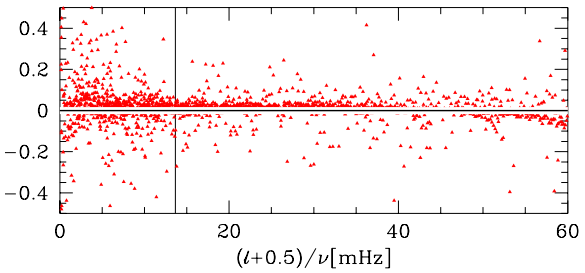

Fig. 3.— Residuals of $\gamma_{\ell n}$ for p-modes after removing the $\gamma_7(\nu)$ fit (see Fig. 2) plotted against position of the lower turning point. The value $(\ell + 0.5)/\nu = 50$ corresponds to depth of 40 Mm. The vertical line indicates the bottom of the convective envelope.

4. Variational expressions for γ

Hamilton's variational principle is our tool for interpreting the frequency changes. It was employed for instance by GMWK

and by DG, whose integral formulae linking the γ's to changes in the magnetic field, turbulent pressure and temperature are used in the present paper. The approach adopts an adiabatic approximation for oscillations, which may not be fully justified in the part of the outer layers of our interest. DG also provided expressions for calculating frequency splittings represented by the even-a coefficients. Here we give a summary of only the formulae that are relevant for calculating the centroid frequencies.

The underlying variational expression for the angular frequency, $\omega(= 2\pi\nu)$, shift used here is

$$\Delta\omega = \frac{\Delta(D_p + D_M + D_v)}{2I\omega}. \qquad (2)$$

The quantities D_p, D_M, and D_v represent contributions of pressure, magnetic field, and turbulent velocity, respectively, to mode frequency. The quantity

$$I = \int d^3\boldsymbol{x}\rho|\boldsymbol{\xi}|^2 \qquad (3)$$

is the mode inertia and $\boldsymbol{\xi}$ is the Lagrangian displacement vector calculated in a standard spherical model. Here we have ignored terms resulting from changes in gravity and large scale velocity fields, since both were found to be negligible.

Only the rms values averaged over spherical surfaces contribute to the changes in the mean frequencies, $\bar{\nu}$. The pressure term may be written in the form

$$D_p = \int d^3\boldsymbol{x}p[\Xi + (\Gamma - 1)|\mathrm{div}\boldsymbol{\xi}|^2], \qquad (4)$$

where $\Xi = \xi^*_{j;k}\xi_{k;j}$ and ";" denotes the covariant derivative. The Lagrangian change of D_p, which is calculated with $\delta(\rho d^3\boldsymbol{x}) = 0$, requires evaluation of the pressure and density perturbations, δp and $\delta\rho$ respectively, induced by changes in the magnetic fields and correlated changes in the turbulent velocity. Such changes arise from the magnetic field's inhibiting of convection. For the spherically symmetrical part of perturbation considered here, the density perturbation is not determined by the condition of mechanical equilibrium. Here, following DG, we express $\delta\rho$ in terms of δp and the Lagrangian temperature perturbation, δT. We treat changes in the magnetic field, turbulent velocity, and temperature as independent sources of frequency changes, even though they are physically linked. Modeling the effect of magnetic field on convection is still not well understood and our approach is to use simple reliable physics to derive helioseismic constraints on advanced models.

Both the magnetic and velocity fields are treated as being statistically random with the net effect on radial structure resulting from their square averaged components. The vertical component was allowed to be different from the two horizontal components. Thus, the covariance matrix for the magnetic field is written in the following form,

$$\begin{aligned}\overline{B_iB_j} &= \delta_{ij}[\delta_{jr}\mathcal{M}^V(r) + \\ &\frac{1}{2}\mathcal{M}^H(r)(\delta_{j\theta} + \delta_{j\phi})], \qquad (5)\end{aligned}$$

where δ_{ij} is the Kronecker symbol. We will use an unsubscripted δ to denote the Lagrangian changes in solar depth dependent parameters, while Δ refers to changes in the global parameters. An analogous form was adopted for the turbulent velocities.

$$\overline{\rho v_i v_j} = \rho\delta_{ij}[\delta_{jr}\mathcal{T}^V_k(r) +$$

$$\frac{1}{2}\mathcal{T}_k^H(r)(\delta_{j\theta}+\delta_{j\phi})]. \qquad (6)$$

Upon assuming mechanical equilibrium in a thin layer, DG (see also GMWK) calculated the change in pressure, δp, resulting from changes in the random magnetic field ($\delta\mathcal{M}^V$, $\delta\mathcal{M}^H$) and in the random velocities ($\delta\mathcal{T}^V$, $\delta\mathcal{V}^H$). The evaluation of the density change requires consideration of the thermal balance. DG calculated ΔD_p assuming an isothermal response of the layer and separately evaluated the contribution to the γ's from the temperature change, δT.

The total dynamical effect of the magnetic field change on frequencies consists of ΔD_p calculated with $\delta T = 0$ and

$$\Delta D_M = \frac{1}{4\pi}\Delta\Big\{\int d^3\boldsymbol{x}\Big[|(\boldsymbol{B}\cdot\boldsymbol{\nabla})\boldsymbol{\xi}|^2 - 2\mathrm{div}\boldsymbol{\xi}^*\boldsymbol{B}\cdot(\boldsymbol{B}\cdot\boldsymbol{\nabla})\boldsymbol{\xi} + \frac{1}{2}|\boldsymbol{B}|^2(\Xi+|\mathrm{div}\boldsymbol{\xi}|^2)\Big]\Big\}. \qquad (7)$$

These two terms combined in Eq. 2 lead to the following expression for γ,

$$\gamma_M = \int d\left(\frac{d_{\rm phot}}{1\ {\rm Mm}}\right)\left[K^V_{M,0}\left(\frac{\delta\mathcal{M}^V}{1\ {\rm kG}^2}\right) + K^H_{M,0}\left(\frac{\delta\mathcal{M}^H}{1\ {\rm kG}^2}\right)\right] \quad \mu\ {\rm Hz}, \qquad (8)$$

where $d_{\rm phot}$ denotes the depth beneath the photosphere. The explicit expressions for $K^V_{M,0}$ and $K^H_{M,0}$ in terms radial eigenfunctions of the mode are given in Eq.(67) of DG. For the case of f-modes we have $K^V_{M,0} \approx \frac{4}{3}K^H_{M,0} > 0$. For p-modes we have $K^V_{M,0} \gg |K^H_{M,0}|$. Fig 4 shows examples of the kernels,

$$K^i_{M,0} = \frac{1}{3}(K^V_{M,0} + 2K^H_{M,0}),$$

for calculating γ due to isotropic changes in the field.

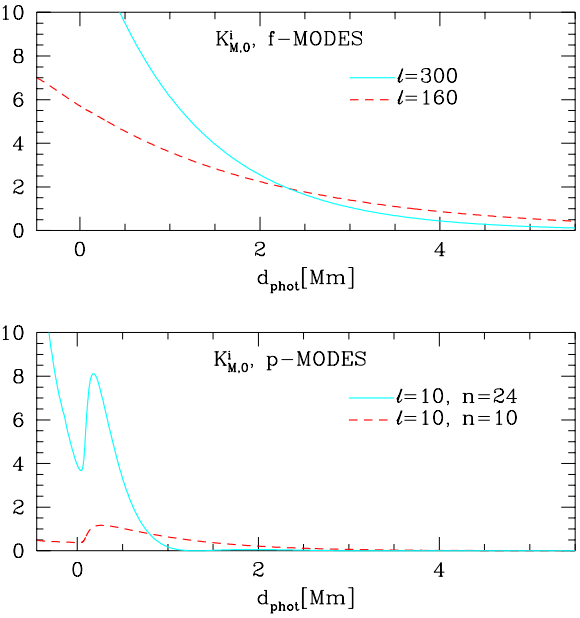

Fig. 4.— Kernels for calculating the γ's arising from isotropic changes in the magnetic field according to Eq. 8, for two selected f-modes (upper panel) and p-modes (lower panel), and at two selected frequencies, are plotted as functions of depth beneath the photosphere in the outer part of the standard solar models.

Comparing the kernels for the two f-modes shown in Fig. 4 with the behavior of the $\gamma(\nu)$ shown in the upper panel of Fig. 2, we conclude that, if the rise of the magnetic field were responsible for the f-mode frequency increase, the growth must occur predominantly beneath 2.5 Mm. The kernels for the p-modes plotted in the lower panel of Fig.4 were calculated for $\ell = 10$. However, in these outermost layers the kernels of all p-modes in the sample are virtually ℓ-independent. The two kernels have very low values at depths beneath 2.5 Mm. It is thus clear that the observed p- and

f-mode frequency increases cannot be simultaneously explained by an increase in the magnetic field. This conclusion does not depend on the assumed isotropy of the field. Isotropy would have been an essential assumption if the field were the cause of the p-mode frequency rise.

The plots in Fig. 5. illustrate the large differences between p- and f-modes kernels at the same frequency. We see that that the f-modes in the MDI sample are far more sensitive to magnetic field changes in outer few Mm below photosphere than the p-modes. We should also note a significant difference between p_1 and the higher order p-modes above $d_{\rm phot} = 1$ Mm. This difference, however, has virtually no consequence because data on p_1 and even p_2 modes are irrelevant for probing this outermost layer.

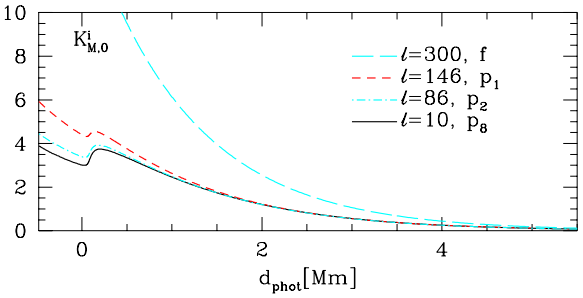

Fig. 5.— Similar to Fig. 4 but for modes of nearly same frequency of $\nu = 1.74$.

The overall dynamical effect of the turbulent velocity changes is calculated in a similar way to that for the magnetic field. To the induced change of D_p calculated assuming $\delta T = 0$, we add the change in the velocity term,

$$\Delta D_v = -\Delta\Big[\int d^3\boldsymbol{x}\rho|(\boldsymbol{v}\cdot\boldsymbol{\nabla})\boldsymbol{\xi}|^2\Big]. \quad (9)$$

When these two terms are used in Eq. 2, we get, after integration over spherical surfaces,

$$\gamma_v = \int d\left(\frac{d_{\rm phot}}{1\ {\rm Mm}}\right)\left[K_v^V\left(\frac{\delta\mathcal{T}^V}{1\ {\rm km^2 s^{-2}}}\right) + K_v^H\left(\frac{\delta\mathcal{T}^H}{1\ {\rm km^2 s^{-2}}}\right)\right] \quad \mu\ {\rm Hz}. \quad (10)$$

Again we do not give expressions for $K^V_{v,0}$ and $K^H_{v,0}$ here. They were given in Eq.(59) of DG. In that paper, we plotted the kernels $K^V_{v,k}$ and $K^H_{v,k}$, with $k = 0$ referring to the centroid changes and $k > 1$ to the even-a coefficients. Unfortunately, there was a numerical mistake in those plots. The plotted kernels were too large by a factor of about 9. In Figure 6, we plot corrected kernels for γ due to changes in the vertical component of the velocity for the same four modes that were selected for use in Fig. 4. The absolute values of the $K^H_{v,0}$ are smaller (factor $\frac{1}{4}$ for the f-modes, and much less than that for the p-modes).

A decrease in the vertical component of the turbulent velocity remains the most viable explanation of the dominant part of the p-mode frequency increase correlated with the magnetic activity cycle because high frequency modes preferentially sample the layers, where we expect the largest changes in the turbulent velocity.

The decrease in the velocities also means a decrease in the efficiency of convective energy transport, hence a decrease of temperature in the outer layers. As GMWK first observed, an isobaric increase of temperature causes an increase in p-mode frequencies. The same is true for f-modes, but there the effect is much smaller. We express the γ's due to the Lagrangian change in temperature, δT, in the form

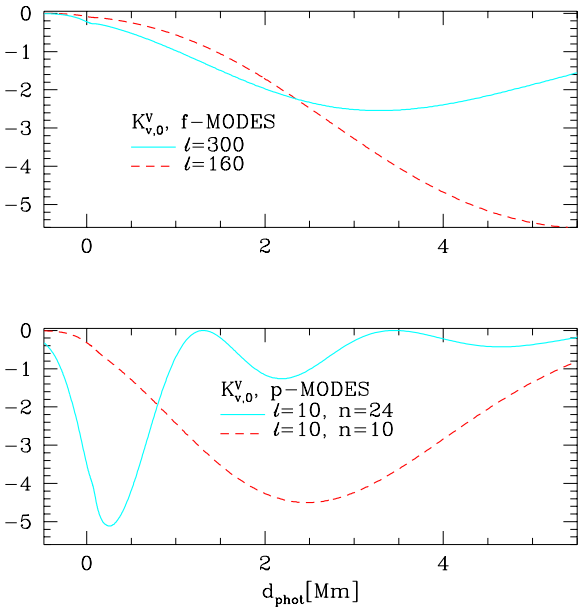

Fig. 6.— Kernels for calculating γ's arising from the change in the random velocity field according to eq. 10 for two selected f-modes (upper panel) and p-modes (lower panel) and at two selected frequencies plotted as functions of depth in outer part of the standard solar models.

$$\gamma_T = \int d \left(\frac{d_{\rm phot}}{1{\rm Mm}} \right) K_T \frac{\delta T}{T} \quad \mu{\rm Hz}, \quad (11)$$

again referring readers to DG for an explicit expression for K_T. The plots of K_T for the same four modes as in Fig. 6 are given in Fig. 7. Here we also decreased the values by a factor of about 1/9 relative to corresponding plots in DG. The kernel's behavior is similar to that seen in Fig. 6. In the shallow subphotospheric layers, where we may expect the largest relative changes of temperature caused by decreased efficiency of convective transport, only p-modes have substantial amplitudes, and it is only for these modes that a temperature decrease must be considered to be a potentially important contributor to the frequency increase.

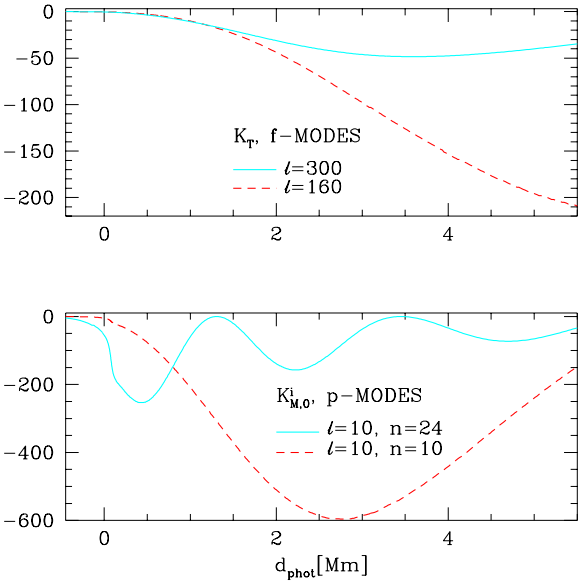

Fig. 7.— Kernels for calculating the frequency shifts due to temperature increase for p-modes at selected frequencies (lower panel) and f-mode modes at selected degrees (upper panel).

5. Changes in subphotospheric magnetic field from changes in the f-mode frequencies

The dynamical effect of the rise of the magnetic field seems to be the only possible explanation for the observed f-mode frequency increases. Formally, one may explain the behavior of the $\gamma(\nu)$'s seen in Fig. 2 in terms of a decrease in the turbulent velocity, but the decrease would have to be nearly constant with depth, and the amount would have to be unacceptably large at depths greater than say 2 Mm.

Probing the depth dependence of the magnetic field based on f-modes has modest precision. Modes in the [180, 300] ℓ-range, for which we have a significant determination of γ, effectively sample the

magnetic field down to a depth of only a few (5-6) Mm, but the probing precision is not high because of the spread in the individual frequency shifts. As a first attempt, we seek the isotropic field change, $\delta(B^2) = \delta(\mathcal{M}^V + \mathcal{M}^H)$, in the form of a truncated power series of the depth below the temperature minimum, $d_{\rm min} = d_{\rm phot} + 0.476$ Mm,

$$\delta(B^2) = \sum_{k=0} \delta(B^2)_k d_{\rm min}^k. \qquad (12)$$

Including terms up to $k = 2$ enabled us to reach similar values of χ^2 to those of the three-term Legendre polynomial fit of the $\gamma(\nu)$ dependence. The resulting $\delta(B^2)(d_{\rm min})$ dependence does not look realistic because we found $\delta(B^2) < 0$ near the photosphere (see curves denoted M1 in Fig. 8), as though the near-surface field decreases with rising activity. With this in mind, we tried a form of the $\delta(B^2)(d_{\rm min})$ function forcing $\delta(B^2) \geq 0$ everywhere. We chose

$$\delta(B^2) = \begin{cases} \delta(B^2)_{\rm int} & \text{if } d_{\rm min} \geq d_{\rm int} \\ \delta(B^2)_{\rm int} \left(\frac{d_{\rm min}}{d_{\rm int}}\right)^j & \text{if } d_{\rm min} \leq d_{\rm int} \end{cases}, \qquad (13)$$

with adjustable parameters $\delta(B^2)_{\rm int}$, $d_{\rm int}$, and j. The lowest χ^2 of 1.69 was reached at $d_{\rm int} = 4$ Mm and $j > 20$ (M2 in Fig.8). However, similar values of χ^2 were reached at higher $d_{\rm int}$ and lower j. One such example (M3) is shown in Fig. 8.

We see that a concave shape of $\gamma(\nu)$ is reproduced only with the model allowing $\delta(B^2) < 0$, but we do not regard this finding to be significant. Rather, we would blame some inadequacy in our model of the small-scale field in the atmosphere.

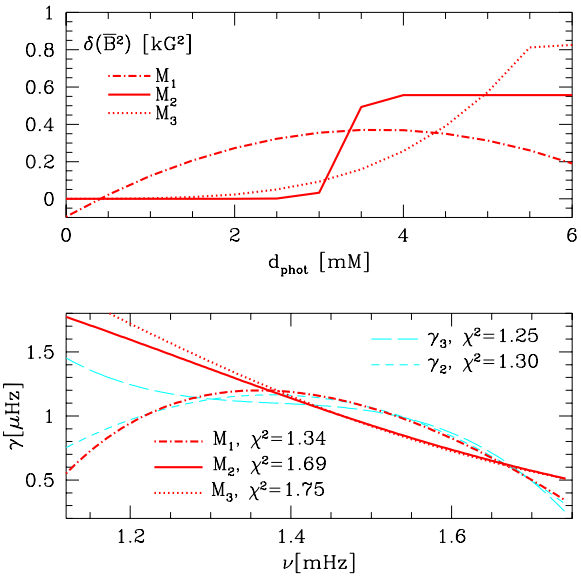

Fig. 8.— The upper panel shows the depth dependence of the mean square field change between solar maximum and maximum for models M1, M2, and M3. The errors in individual values of $\delta(\bar{B}^2)$ for the M1 model are large, growing from 0.03 at $d_{\rm phot} = 0$ to 0.3 (kG)^2 at $d_{\rm phot} = 5.5$ Mm. In the lower panel, the bolder lines show that the γ's calculated for each of the three models. The thinner lines show $\gamma(\nu)$ functions obtained by fitting truncated Legendre polynomial series as described in Section 3.

What we regard to be significant is that the f-mode frequency increase between solar minimum and maximum requires an average field increase of some 0.5 - 0.7 kG at a depth of about 5 Mm and a much smaller increase close to the photosphere.

6. The dominant source p-mode variations

Changes in the magnetic fields inferred from f-mode data have only a very small effect on p-mode frequencies. This is illustrated in Fig. 9 where in the lower panel we show the 7th-order Legendre polynomial fits of the measured frequency difference after removing the effect of the field according to model M2. Only in the lower frequency section, below $\nu = 2$ mHz, are the increases in the γ's with decreasing ν reduced. This suggests that the averaged dynamical effect of the magnetic field rise at a depth of a few Mm is responsible for an appreciable part of the frequency increase of low frequency p-modes. However, we should stress that, as we may see in Fig. 2, the significance of $\gamma(\nu)$ in this part of the p-mode spectrum is questionable. In any case, most of the p-mode frequency increase with rising activity requires a different explanation.

The high frequency part of the $\gamma(\nu)$ dependence, which is really significant, may be explained only by invoking an effect acting preferentially close to the sun's photosphere. The dynamical effect of the growing magnetic field is excluded by measurements of the averaged photospheric field and by the f-mode data. What remains to be considered is an inhibiting effect of the field on convection leading to a lower turbulent velocity and temperature in the outermost layers. The two effects are expected to be significant only close to the photosphere. The question to answer is how much of a reduction is required to account for the observed frequency changes.

We first consider the effect of lowering the turbulent velocity. In fact, only the vertical component of it matters because the horizontal components hardly affect p-mode frequencies. The squared averaged vertical velocity in Eq. (9) is represented in the form of a truncated power series of the depth beneath the temperature minimum, $d_{\rm min}$,

$$\delta(\mathcal{T}^V) = \sum_{k=0} \delta(\mathcal{T}^V)_k d_{\rm min}^k. \qquad (14)$$

It turned out that it suffices to include terms up to $k = 2$ to fit the measured γ's with a χ^2 better than that from the seventh order polynomial $\gamma(\nu)$. The fits are compared in the lower panel of Fig. 9.

In the upper panel of Fig. 9, we show the inferred $\delta(\mathcal{T}^V)(d_{\rm phot})$ dependence with the 1σ error bars from the least square fit. The changes required to account for the p-mode frequency rise are naturally higher than those assessed by DG, as the kernels they used were grossly exaggerated (by about a factor of nine due to an error, which has been fixed here), but the crude estimate made therein results in an error that is smaller than should have been expected. With our present corrected and precise analysis, we get higher numbers but they are not unreasonably high. The comparison with the model values shows that what is required is less than a 2.5 % decrease in $\mathcal{T}^V$ that is a less than 1.3% decrease in the rms vertical component of the turbulent velocity. We do not believe this number is in conflict with observations.

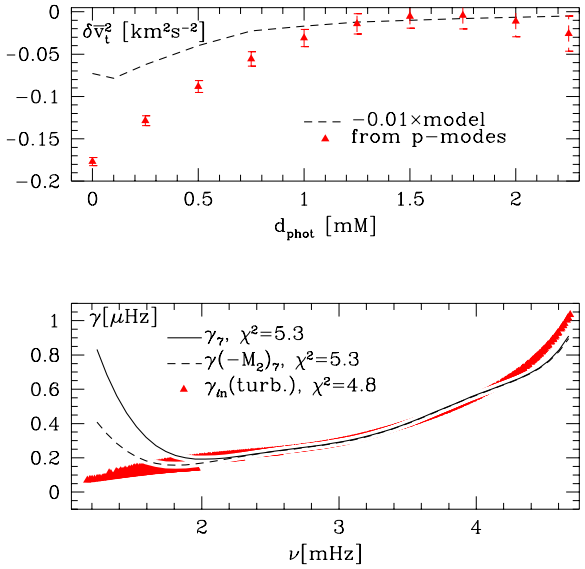

Fig. 9.— Continuous lines in the lower panel show $\gamma(\nu)$ functions obtained by fitting the Legendre polynomial dependence to measured p-mode frequency shifts with and without removing the effect of magnetic field changes according to model M2 (see upper panel of Fig. 8). Symbols denote individual values of $\gamma_{\ell n}$ calculated assuming that the p-mode frequency shift is caused by a decrease in the turbulent velocity. The upper panel shows the inferred values of the change in the mean squared turbulent velocity and compares them with the 1 percent decrease of those values calculated in a model of the solar convective zone of Abbett et al. (1997).

A potentially more difficult problem arises from implication of the reduced convective efficiency on the effective temperature. According to a crude estimate, based on mixing-length approximation and an Eddington atmosphere given by DG, a 1 percent decrease in the convective velocity is associated with a relative temperature decrease ranging from 1×10^{-3} at $d_{\rm phot} = 1$ to 3×10^{-3} at $d_{\rm phot} = 0$ Mm. The values are about one half of what is needed to account for the p-mode frequency increase solely by the temperature effect. Thus, the required velocity reduction is smaller but even with that the implied decrease in the effective temperature of some 7 K seems unacceptably high. Nonetheless, we believe that the inhibiting effect of the magnetic field on convection is the cause of p-mode frequency increase correlated with increasing activity. We cannot conceive of a more plausible explanation, and we blame the problem regarding the effective temperature change on inadequacies in our treatment of energy transport in the convective zone and in the atmosphere.

7. Conclusions

We analyzed all available SOHO/MDI data to study the behavior of the mean solar frequencies with varying magnetic activity. Averaged over their respective frequency ranges, the time variations of p- and f-mode frequencies show the same pattern. Both are strictly correlated with sunspot number. The difference is seen when the mode dependence of the frequency shifts between activity maximum and minimum is compared. The quantities we compare are the shifts scaled by mode inertia, that is the γ's. There is a slight

residual mode dependence for p-modes indicating that there is a contribution to the shift arising in deeper layers, but still well above the bottom of the convective envelope. In the frequency ranges where $\gamma(\nu)$ is well determined, the two types of modes exhibit opposite trends with increasing frequency: growing γ's for p-modes and declining ones for f-modes. We determined different scenarios as the explanation of the dominant source of the frequency changes in these two cases.

We considered two possible sources of the mean frequency changes (1) dynamical effects of the changing, average, small-scale magnetic field (2) effects of turbulent velocity and subphotospheric temperature changes caused by the impeding effect of the field on convection. In our analysis, we relied on formalism developed by DG. We also revised some estimates presented in that work.

We demonstrated that the main part of the f-mode frequency shifts is explained by the growth of the subphotospheric magnetic field. The relevant growth takes place in the layers at depths of 2.5-5 Mm rising to about $0.5-0.7$ kG. The detailed implications regarding both shallower and deeper layers are uncertain. Formally, the best fit is obtained if there is a slight decrease in the mean photospheric field in the outermost layer with increasing activity, but we do not believe that this is realistic beyond saying the field growth there is small.

Because of its location, the field causing f-mode frequency rise has only a minor effect on p-modes. The weak field rise in the outermost layers is also consistent the direct measurements of the mean photospheric field (Lin 1995, and Lin and Rimmele 1999). This outermost layer is where the dominant source of the frequency p-mode change resides. Thus, we can exclude the field as the source of p-mode changes. Attributing the p-mode frequency shifts to a decrease in turbulence, we found that this requires less than a two percent decrease in the rms value of the vertical component, as calculated in a model of solar convection. Impeded convective flows also cause lower temperatures in the outermost convective layers. Lowering the temperature causes frequency rise because the effect of cooling is more than compensated by the resulting contraction.

The difficulty of the proposed explanation of the p-mode frequency shifts comes from the implied decrease of the effective temperature by some 7K between solar minimum and maximum phase. Since our estimate is based on a very crude model, we do not regard this problem as essential but we think it calls for a closer study with advanced models of the convective zone and atmosphere of the sun.

Let us return to the question posed in the title of the DGS paper: *Does the sun shrink with increasing magnetic activity?* The answer following from our present analysis is: yes, it does. Changes at depths beneath 8 Mm in depth, which were previously suggested to amount to about 1.5 km per year during the rising activity phase, are most likely negligible. The dominant effect influencing mass distribution in the outermost layers is the decrease of the turbulent pressure and temperature with increasing activity, and both effects cause shrinking. The implied shrinking amounts to about 1 km between solar minimum and maximum. The roughly 1% decrease of the

squared turbulent velocity in the outer 1 Mm below the photosphere must be compensated by a 0.1 percent density rise because turbulence contributes about 10 percent of the total pressure. We would obtain the same estimate of the shrinking by attributing part of the p-mode frequency increase to the temperature decrease.

A cooler and smaller active sun, whose increased irradiance is totally due to activity induced corrugation, has been advocated for years by Spruit (e.g. 1991, 2000). Our results support his picture.

This research was supported in part by a Polish grant (KBN-5 P03D 030 20), U.S. grants from NASA (NAG5-12782) and NSF (ATM-0342560). We thank the SoHo/MDI team, Jesper Schou in particular, for easy access to their fine data.

REFERENCES

Abbet, W.B, Beaver, M., Davids, B., Georgobiani, D., Rathbin, P., & Stein, R.F. 1997, ApJ, 480, 395

Antia, H.M., Basu, S., Pintar, J. & Pohl, B. 2000, Solar Phys., 192, 459

Antia, H.M. 2003, ApJ, 590, 567

Bachmann, K., & Brown, T. 1993, ApJ, 411, L45

Chaplin, W. J., Elsworth, Y., Isaak, G. R., Lines, R., McLeod, C. P., Miller, B. A., & New, R. al. 1998, MNRAS, 300, 1077

Christensen-Dalsgaard, J., Däppen, W., Ajukov, S.V., et al. 1996, Science, 272, 1286

Dziembowski, W. A. & Goode, P. R. 2004, ApJ, 600, 464 (DG)

Dziembowski, W. A., Goode, P. R., & Schou, J. 2001, ApJ, 553, 897 (DGS)

Elsworth, Y.; Howe, R.; Isaak, G. R.; McLeod, C. P.; Miller, B. A.; New, R.; Speake, C. C.; Wheeler, S. J. 1994, ApJ, 434, 801.

Goldreich, P., Murray, N., Willette, G., & Kumar, P. 1991, ApJ, 370,752 (GMWK)

Kuhn, J.R. 2000, Space Sci.Rev., 94, 177

Libbrecht, K. G., & Woodard, M. F. 1990, Nature, 345, 779

Lin, H. 1995, ApJ, 446, 421

Lin, H. & Rimmele, T. 1999, ApJ, 414, L448

Regulo, C.; Jimenez, A.; Palle, P. L.; Perez Hernandez, F.; Roca Cortes, T. 1994, ApJ, 434, 384.

Spruit, H.C. 1991 in *The Sun The Time*, eds. Sonett, C.P., Giampappa, M.P., & Matthews, M.S., University of Arizona Press, p. 118

Spruit, H.C. 2000, Space Sc. Rev, 94, 113

Woodard, M., & Noyes, R. 1985, Nature, 318, 449.

Woodard, M., Kuhn, J., Murray, N., & Libbrecht, K. 1991, ApJ, 373, L81

This 2-column preprint was prepared with the AAS LaTeX macros v5.0.